DEVELOPMENT OF AN SU-8 FABRY-PEROT BLOOD PRESSURE SENSOR

R. Melamud[1], A.A. Davenport[1], G.C. Hill[2], I.H. Chan[3], F. Declercq[4], P.G. Hartwell[5], B.L. Pruitt[1]
Departments of [1]Mechanical Engineering, [2]Applied Physics, and [3]Medicine
Stanford University, Stanford, California, USA
[4]Section de Microtechnique, Ecole Polytechnique Federale de Lausanne, Lausanne, Switzerland
[5]Hewlett-Packard Laboratories, Palo Alto, California, USA

ABSTRACT

This paper presents the fabrication method and testing of an interferometric pressure sensor designed for intravascular blood pressure measurements. A cap containing a pressure-sensing diaphragm was mounted onto the end of a fiber optic cable. The Fabry-Perot interferometer, formed between the reflective diaphragm and the fiber's end, measured the diaphragm deflection. Microfabricated from the biocompatible polymer, SU-8, the device is fast, simple, and inexpensive to manufacture. Its small dimensions (<300μm outer diameter) reduce the risk of infection and thrombosis and allow for its insertion into small vessels. The sensor showed a linear response to pressure from 0 to 125 mmHg with approximately 1-2 mmHg resolution. The use of an optical displacement transducer allowed a series of careful measurements of drift and hysteresis of SU-8 materials in different environments. This data may be valuable to other researhcers working with SU-8.

1. INTRODUCTION

Fabry-Perot interferometers (FPI) have been successfully employed as sensors of strain, temperature, pressure, and displacement. FPI sensors are exquisitely sensitive to changes in optical path length, yet immune from electrical interference. A common pressure measurement scheme, used in the device presented here, incorporates a diaphragm that deflects under pressure at one end of an FPI cavity. A variety of diaphragm designs have been reported, including a silicon-micromachined mesa[1], a dipped polymer membrane[2], and a bonded silicon membrane[3].

The potential medical applications for fiber optic sensors have long been recognized. Invasive blood pressure measurements provide critical diagnostic information but carry risk of thrombosis, embolism, and infection. Fluid-filled catheters are currently used, but damp blood pressure dynamics and are too large and hazardous for some situations. Other researchers have reported using a gas bubble at the tip of a fiber optic cable for medical FPI pressure measurements[4]. More recently, a silicone membrane fused to Pyrex has been tested *in vivo* as a non-invasive intraocular pressure sensor[5].

The device presented here consists of an SU-8 cap that fits onto a fiber optic cable (Figure 1). SU-8 is an epoxy-based photoresist that cures into a glassy, biocompatible material[6]. Features with high aspect ratios can be fabricated from SU-8 using conventional photolithography. SU-8 is easier and less expensive to micromachine than silicon. With a lower elastic modulus, SU-8 also deflects more than silicon for a given pressure, resulting in improved pressure sensitivity. A similar concept was recently described in a patent[7], but this is the first presentation of fabrication and results for a working SU-8 FPI device.

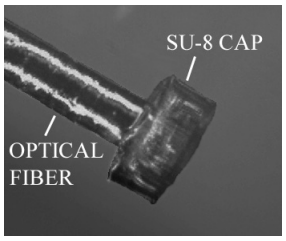

Figure 1: Photograph of sensor.
300 μm-wide SU-8 cap on a 125μm fiber optic cable.

2. DESIGN

The cavity formed between the fiber's end and the diaphragm acts as an FPI sensor. When illuminated with broadband light, the reflection from the cap is the source spectrum modulated by the characteristic Airy interference pattern (Figure 2). Minima in the reflected light spectrum occur at wavelengths that build up standing waves in the FPI cavity by constructive interference. These wavelengths are proportional to the cavity length. A change in cavity length, dL, produces a shift in the wavelength of a particular minima, $d\lambda_n$, given by:

$$d\lambda_n = \frac{2}{n} dL \tag{1}$$

where n is the integer number of half-wavelengths in the cavity. The wavelengths of reflectance minima were interpolated from a given interference spectrum after

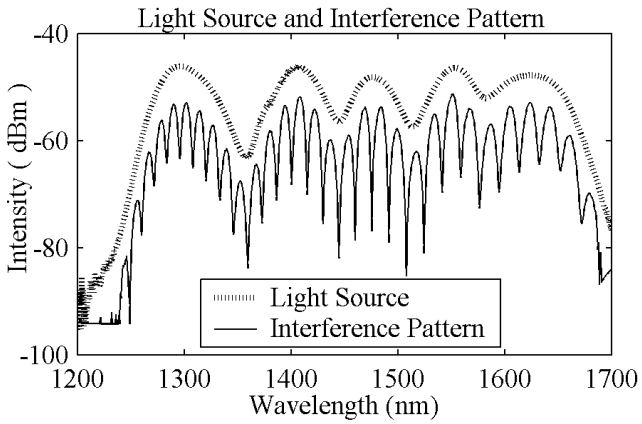

Figure 2: Light source spectrum and typical reflection pattern. Reflection mimics the broad spectral features of the source, but modulated by sharp interference minima.

correcting for the spectral features of the light source. The wavelength shift of a particular minimum between two different spectra was used to extract the corresponding change in cavity length.

Using the analytical expression for small deflections of a clamped circular diaphragm under uniform pressure[8], the change in cavity length is linearly related to change in pressure, *dP*:

$$dL = -\frac{3r^4(1-\nu^2)}{16Et^3}dP \approx -3.8[\frac{nm}{mmHg}]dP \qquad (2)$$

using E = 4.95 GPa and ν = 0.22 as the Young's Modulus and Poisson's ratio of SU-8[9], and r = 50 μm and t = 2 μm as the diaphragm's radius and thickness. Thus, pressure change and minima shift should be linearly related.

3. FABRICATION

Devices were fabricated from three layers of SU-8 photoresist (MicroChem) using standard photolithography techniques and the manufacturer's processing recommendations (Figure 3). First, a release layer, OmniCoat (MicroChem), was spun onto a handle silicon wafer. A 2 μm-thick layer of SU-8 2 formed the diaphragm, while a second layer of SU-8 2035, approximately 50 μm-thick, formed the cylindrical wall around the cavity of the interferometer. A sleeve that sheathes the fiber was made from a 100 μm-thick layer of SU-8 100. The fiber sleeve layer contained a hole wider than the fiber diameter of 125 μm, while the hole in the cavity layer was smaller to act as an insertion stop for the fiber. A 3 minute, 80 W oxygen plasma etch was used to roughen the surfaces of and increase adhesion between SU-8 layers. To enhance reflection from the diaphragm, metal was evaporated onto the entire wafer. Devices were coated with 200 Å of chromium followed by 1000 Å of titanium. After developing the release layer, micromanipulators were used to insert the cleaved end of a single mode fiber into the cap. The cap was secured and sealed with biocompatible cyanoacrylate glue.

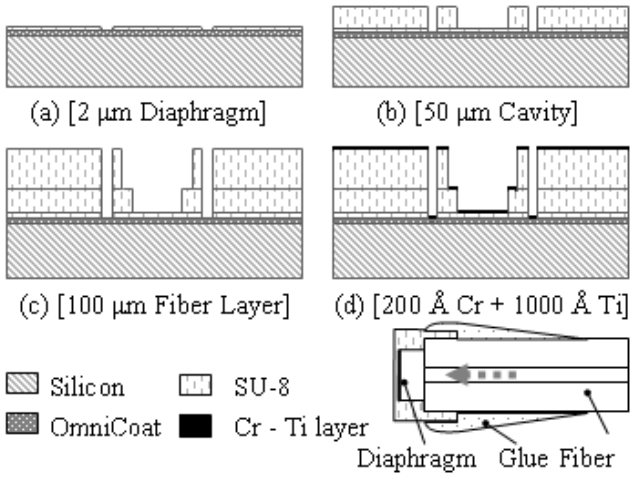

Figure 3: Fabrication process of an SU-8 cap and final assembly.

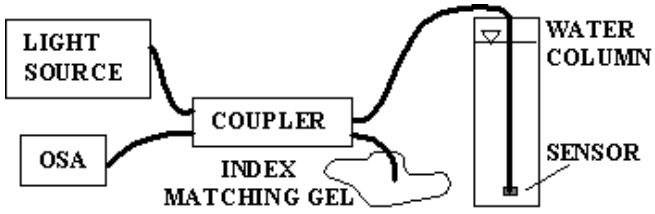

Figure 4: Experimental Set-Up. Broadband light source illuminated the sensor through a fiber coupler. An optical spectrum analyzer (OSA) recorded the reflected spectrum.

4. EXPERIMENTAL SET-UP

A 3 dB fiber coupler connected an infrared superluminescent diode light source (B&W Tek SLD-15) to the sensor (Figure 4). An optical spectrum analyzer (Agilent 86140B) measured the reflected spectrum. Index-matching gel was used to eliminate reflection from the extra end of the coupler. For pressure experiments, the device was submerged in a vertical column of deionized (DI) water to create a pressure difference across the diaphragm.

5. RESULTS

The sensor's response to pressure changes was tested by adjusting its depth in a water column and analyzing the reflected spectrum (Figure 5). Prior to the experiment, the sensors were left in DI water to equilibrate. Measurements began near atmospheric pressure (labeled 0 mmHg) and increased to 125 mmHg before decreasing back to 0 mmHg. Consistent with theory, cavity length decreased linearly with increasing pressure. The observed sensitivities (–1.8 to –2.8 nm change in cavity length per mmHg) are within the uncertainty of the material properties and dimensions used to calculate the theoretical sensitivity, –3.8 nm per mmHg. Slight non-linearity and hysteresis in the plots suggest that other variables in addition to pressure affect the sensors' cavity lengths.

The long-term drift in cavity length and sensitivity to pressure can be seen in Figure 6. Pressure response measurements for three sensors were repeated over several days. During that time, the sensors were continuously immersed in water, but not always exposed to the light source. Over time, the sensor's absolute sensitivity decreased, and the relationship between pressure and cavity length became more non-linear.

This behavior might be due to modest temperature fluctuations in the laboratory (2-3°C), or to fluctuations in SU-8's water absorption due to other environmental factors. Several experiments were conducted to explore the sources of drift in the pressure measurements.

Cavity length drift was measured in air, water, and saline. The devices in air (Figure 7a) experienced decreasing cavity lengths for approximately two and a half hours after initial exposure to the light source. This shrinking was possibly due to ongoing cross-linking of the SU-8 polymer. The several milliwatts of optical power incident on the device from the light source could be heating the sensor.

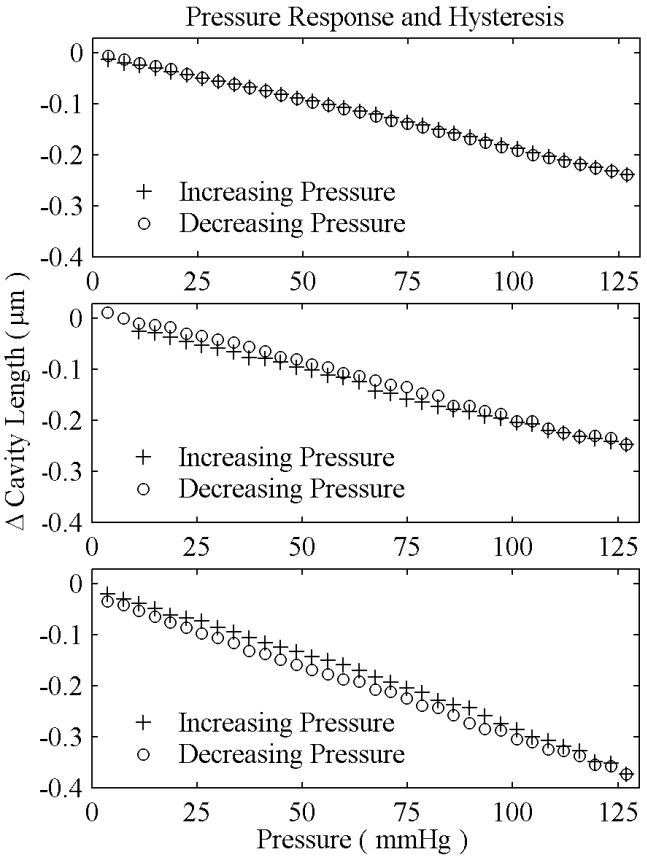

Figure 5: Cavity length decreased linearly with increasing pressure for three sensors. Measurements began by increasing pressure from atmospheric (labeled 0) to 124 mmHg, and then decreased back to 0 mmHg over 1 hour. Slight non-linearity and hysteresis reveal long-term drift.

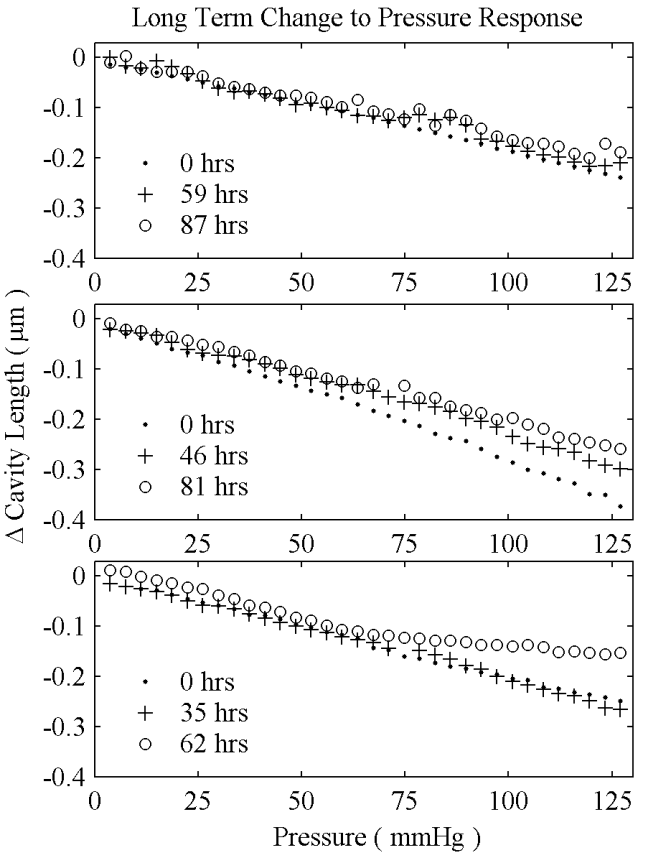

Figure 6: Response to pressure for three devices, repeated over several days. Sensitivity decreased and non-linearity increased with time.

After stabilization in air, six devices were immersed into a temperature controlled 30°C bath of DI water (Figure 7B) or saline solution (Figure 7C). In both liquids, the sensors underwent rapid changes in cavity length after immersion. Immersion in water caused elongation of the cavities, sometimes followed by a milder relaxation. The cavity lengths leveled off after expanding from 0.75 μm to 1.5 μm relative to their original lengths in air. Cavity length fluctuations were reduced after 3 hours immersion, but still drifted by 20 to 90 nm per hour, as determined by a linear fit to data from the last hour of measurement.

In contrast, the saline caused a period of shrinkage from 10 to 25 minutes after immersion. Each sensor expanded slightly after this nadir, but settled toward lengths ranging from +0.75 μm to –0.75 μm relative to their original length in air. The cavity length of the sensors in saline drifted from –10 to +30 nm per hour after several hours immersion.

One potential cause of the observed cavity length increases is swelling from water absorption. The saline solution might remove moisture or solvents in the SU-8 polymer by osmotic forces and cause shrinkage. Also, some of the drastic, initial behavior might be due to temperature changes, particularly when a sensor was first inserted into a liquid bath.

The effects of temperature on cavity length were characterized for a cap immersed in water (Figure 8). The cavity length increased monotonically with temperature, though the relationship is nonlinear over the full range from 5 ºC to 70 ºC. In the linear region of the plot, between 5ºC and 35ºC, both cavities showed thermal expansion rates of 22 nm per ºC. This expansion is due to both axial lengthening and to the outward bending of the diaphragm from mismatch in the coefficients of thermal expansion for SU-8 and titanium. A finite element model incorporated both these effects and predicted a thermal expansion rate of 15 nm per ºC using the previously listed material properties of SU-8 and α = 52 ppm as SU-8's coefficient of thermal expansion [10]. There is reasonable agreement between the theoretical and experimental expansion rates given the uncertainty in SU-8's material properties.

6. CONCLUSIONS

A fiber optic pressure sensor was fabricated from the polymer SU-8 using a simple, three-mask process. Initial testing showed a linear response to pressure with satisfactory resolution for intravascular blood pressure measurements. The SU-8 cap was sensitive to swelling and temperature changes, and further work on fabrication parameters should add stability to the device. The sensor also shows promise for measuring blood pressure dynamics.

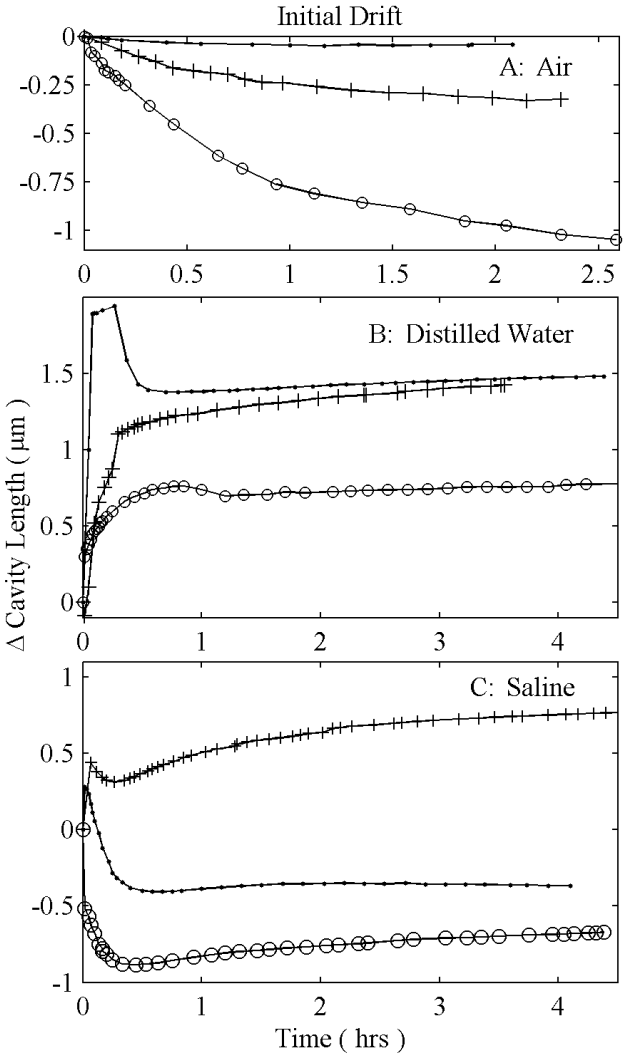

Figure 7: Cavity length change for three sensors in: (a) air (b) distilled water (c) saline. (b) and (c) were previously stabilized in air, while (a) begins with light exposure. Cavities shrink initally when illuminated in air, swell in water, and have mixed responses to saline immersion.

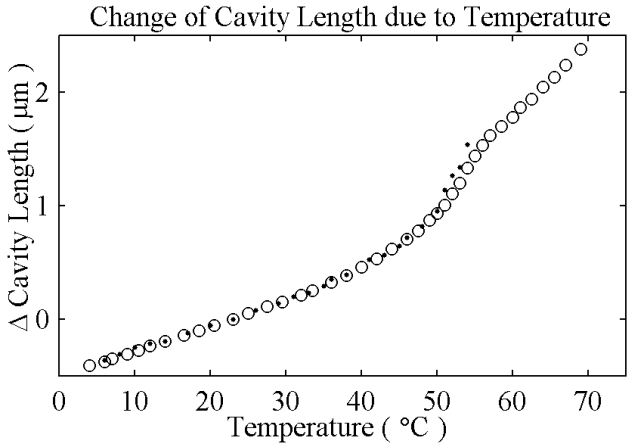

Figure 8: Cavity length increases with temperature. Two devices shown.

ACKNOWLEDGEMENTS

The authors wish to thank the Solgaard, Byer, Kenny, and Miller research groups at Stanford University for their generosity with equipment and expertise. The material presented here was supported by two Stanford Graduate Fellowships and a National Science Foundation Fellowship. Work was performed in part at the Stanford Nanofabrication Facility (a member of the National Nanotechnology Infrastructure Network) which is supported by the National Science Foundation under Grant ECS-9731293, its lab members, and the industrial members of the Stanford Center for Integrated Systems.

REFERENCES

[1] T. Katsumata, Y. Haga, K. Minami, and M. Esashi, "Micromachined 125 um diameter ultra miniature fiber-optic pressure sensor for catheter.," *Transactions of the Institute of Electrical Engineers of Japan, Part E*, vol. 120/E, pp. 58-63, 2000.

[2] E. Cibula, D. Donlagic, and C. Stropnik, "Miniature fiber optic pressure sensor for medical applications.," presented at IEE Sensors 2002, Orlando, FL, USA, 2002.

[3] D. C. Abeysinghe, S. Dasgupta, J. T. Boyd, and H. E. Jackson, "A novel MEMS pressure sensor fabricated on an optical fiber.," *IEEE Photonics Technology Letters*, vol. 13, pp. 993-5, 2001.

[4] S. McClelland, "Optical sensors: smaller, cheaper, faster.," *Sensor Review*, vol. 8, pp. 19-22, 1988.

[5] E. Ahmed, J. Ma, I. Rigas, N. Hafezi-Moghadam, E. Iliaki, E. S. Gragoudas, J. W. Miller, and A. P. Adamis, "Non-Invasive Tonometry in the Mouse.," *ARVO Annual Meeting Abstract Search and Program Planner*, vol. 2003, pp. 3336, 2003.

[6] G. Voskerician, M. S. S. Shive, R. S. S. Shawgo, H. V. R. Recum, J. M. A. Anderson, M. J. C. Cima, and R. Langer, "Biocompatibility and biofouling of MEMS drug delievery devices," *Biomaterials*, vol. 24, pp. 1959-1967, 2003.

[7] H. R. Fetterman, L. Bukshpun, and J. Michael, "Ultraminiature fiber optic pressure transducer and method of fabrication." U.S. Patent 6,506,313: Pacific Wave Industries, Inc., January 14, 2003.

[8] W. C. Young and R. G. Budynas, "Roark's Formula for Stress and Strain," 7 ed: McGraw-Hill, 2002, pp. 488.

[9] L. Dellmann, S. Roth, C. Beuret, G. A. Racine, H. Lorenz, M. Despont, P. Renaud, P. Vettiger, and N. F. de Rooij, "Fabrication process of high aspect ratio elastic structures for piezoelectric motor applications.," presented at Transducers '97, Chicago, IL, USA, 1997.

[10] H. Lorenz, M. Laudon, and P. Renaud, "Mechanical characterization of a new high-aspect-ratio near UV-photoresist," *Microelectronic Engineering*, vol. 42, pp. 371-374, 1998.